Radiative Bistability and Thermal Memory

Viacheslav Kubytskyi, Svend-Age Biehs, Philippe Ben-Abdallah

Radiative Bistability and Thermal Memory

Viacheslav Kubytskyi,[1] Svend-Age Biehs,[2] and Philippe Ben-Abdallah[1,*]
[1]*Laboratoire Charles Fabry, UMR 8501, Institut d'Optique, CNRS, Université Paris-Sud 11, 2, Avenue Augustin Fresnel, 91127 Palaiseau Cedex, France*
[2]*Institut für Physik, Carl von Ossietzky Universität, D-26111 Oldenburg, Germany*
(Received 18 April 2014; published 15 August 2014)

We predict the existence of a thermal bistability in many-body systems out of thermal equilibrium which exchange heat by thermal radiation using insulator-metal transition materials. We propose a writing-reading procedure and demonstrate the possibility to exploit the thermal bistability to make a volatile thermal memory. We show that this thermal memory can be used to store heat and thermal information (via an encoding temperature) for arbitrary long times. The radiative thermal bistability could find broad applications in the domains of thermal management, information processing, and energy storage.

DOI: 10.1103/PhysRevLett.113.074301 PACS numbers: 44.05.+e, 12.20.-m, 44.40.+a, 78.67.-n

The control of electric currents with diodes and transistors is undoubtedly a cornerstone in modern electronics which has revolutionized our daily life. Astonishingly, similar devices which allow for controlling the heat flow are not as widespread as their electronic counterparts. In 2006, Li *et al.* [1] proposed a thermal analog of a field-effect transistor by replacing both the electric potentials and the electric currents in the electronic circuits by thermostats and heat fluxes carried by phonons through solid segments. A few years later, several prototypes of phononic thermal logic gates [2] as well as thermal memories [3,4] have been developed from these basic building blocks allowing for processing information with heat currents rather than with electric currents. However, this phonon-based technology is intrinsically limited by the speed of the heat carriers, the acoustic phonons, and by the presence of Kapitza resistances between the basic solid elements. Moreover, because of radiative losses and thermal fluctuations, the temporal stability of these systems is limited and a frequent refreshing is needed. To overcome these problems, optical contactless analogs of some basic devices such as the radiative thermal diode [5,6] and the radiative transistor [7] have recently been introduced. However, some functionalities are, to date, missing to allow for an all-photonic treatment of heat fluxes.

In this Letter, we make a step forward in this direction by introducing the concept of a radiative thermal memory which is able to store information for an arbitrary long time using thermal photons. To do so, we first demonstrate the existence of bistable thermal behavior in simple systems consisting of two membranes which are out of thermal equilibrium and which are further sandwiched between two thermal baths at different temperatures. The existence of multiple equilibrium temperatures requires [3] the presence of negative differential thermal resistances. However, as shown by Fan and co-workers [8], this is not at all a sufficient condition. As we will show, the thermal bistability mechanism can only exist in many-body systems [9–11]. Finally, as a direct consequence, we show that the bistability can be used to store one bit of thermal information. While, in a conventional electronic memory, the states 0 and 1 are defined by two different applied voltages for which the electric current inside the circuit is 0, its thermal counterpart is defined with distinct equilibrium temperatures which lead to vanishing heat fluxes between the different parts of the system.

Let us consider a system as depicted in Fig. 1 composed by two parallel homogeneous membranes of finite thicknesses δ_1 and δ_2 and separated by a distance d. The left (right) membrane is in contact with a thermal bath having temperature T_L (T_R), where $T_L \neq T_R$. In a practical point of view, the field radiated by these baths can be produced by

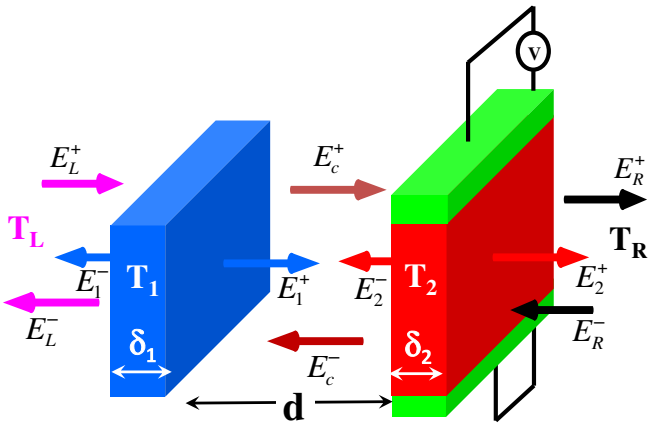

FIG. 1 (color online). Sketch of a radiative thermal memory. A membrane made of an IMT material is placed at a distance d from a dielectric layer. The system is surrounded by two thermal baths at different temperatures T_L and T_R. The temperature T_2 can be increased or reduced either by Joule heating by applying a voltage difference through a couple of electrodes or by using Peltier elements.

external blackbodies. The membranes themselves interact, on the one hand, through the intracavity fields and on the other with the thermal baths, which can be thought to be produced by external media. In that sense, the system is driven by many-body interactions.

The heat flux across any plane $z = \bar{z}$ parallel to the interacting surfaces is given by the normal component of the Poynting vector

$$\varphi(\bar{z}) = \langle \mathbf{E}(\bar{z}) \times \mathbf{H}(\bar{z}) \rangle \cdot \boldsymbol{e}_z. \quad (1)$$

Here, $\boldsymbol{e}_z$ denotes the unit vector normal to the interfaces of the membranes; $\mathbf{E}$ and $\mathbf{H}$ are the local electric and magnetic fields, which, according to fluctuational electrodynamics developed by Rytov and co-workers [12,13], are either generated by randomly fluctuating source currents in both membranes or given by the fluctuational fields of the thermal baths. Here, the angled brackets represent the classical statistical averaging over all field realizations. For the sake of simplicity, we assume that the separation distance d is large enough compared to the thermal wavelengths {i.e., $d \gg \max[\lambda_{T_i} = c\hbar/(k_B T_i)]$, $i = 1, 2, L, R$} so that near-field heat exchanges can be neglected. Then, according to the theory of fluctuational electrodynamics, the heat flux can be written in terms of the field correlators $\mathfrak{C}_j^{\phi,\phi'}(\omega, \boldsymbol{\kappa}) = \frac{1}{2}\langle [E_j^{\phi}(\omega, \boldsymbol{\kappa}) E_j^{\phi'\dagger}(\omega, \boldsymbol{\kappa}) + E_j^{\phi'\dagger}(\omega, \boldsymbol{\kappa}) E_j^{\phi}(\omega, \boldsymbol{\kappa})] \rangle$ of local field amplitudes in polarization j [14]

$$\varphi(\bar{z}) = 2\epsilon_0 c^2 \sum_{\substack{j=s,p \\ \phi=\{+,-\}}} \int_0^{\infty} \frac{d\omega}{2\pi} \int \frac{d^2\boldsymbol{\kappa}}{(2\pi)^2} \frac{\phi k_z}{\omega} \mathfrak{C}_j^{\phi,\phi}(\omega, \boldsymbol{\kappa}), \quad (2)$$

where $\boldsymbol{\kappa} = (k_x, k_y)$ and $k_z = \sqrt{(\omega^2/c^2) - \boldsymbol{\kappa}^2}$ denote the parallel and normal components of the wave vector. The local field and therefore the correlator $\mathfrak{C}_j^{\phi,\phi}$ can be expressed (see Ref. [15] for details) after scattering in terms of fields $E_i^{\pm}$ $(i = 1, 2, L, R)$ emitted by each body and by both thermal reservoirs, as illustrated in Fig. 1. Using expression (2), we can calculate the net flux $\Phi_1 = \varphi(0) - \varphi(-\delta_1)$ $[\Phi_2 = \varphi(d + \delta_2) - \varphi(d)]$ received by the first (second) membrane.

Now, let us assume that one of both membranes, medium 2, say, is made of vanadium dioxide (VO_2), an insulator-metal transition (IMT) material which undergoes a first-order transition (Mott transition [16]) from a high-temperature metallic phase to a low-temperature insulating phase [17] at a critical temperature T_c close to room temperature ($T_c = 340$ K). As shown in Fig. 2, during the phase transition of VO_2 which can be initiated by a small change of its temperature around T_c, the optical properties of VO_2 change drastically. Different works have already shown [6,18] that the exchanged heat flux is drastically affected by this transition. As far as medium 1 is concerned, we use a SiO_2 membrane [19] which is partially transparent in the infrared range. Hence, depending on the crystalline phase of the IMT, the membranes are either under the influence of both thermal reservoirs or mainly of one of them, since the VO_2 layer in its metallic phase is playing the role of a mirror in the infrared, as can be seen in Fig. 2.

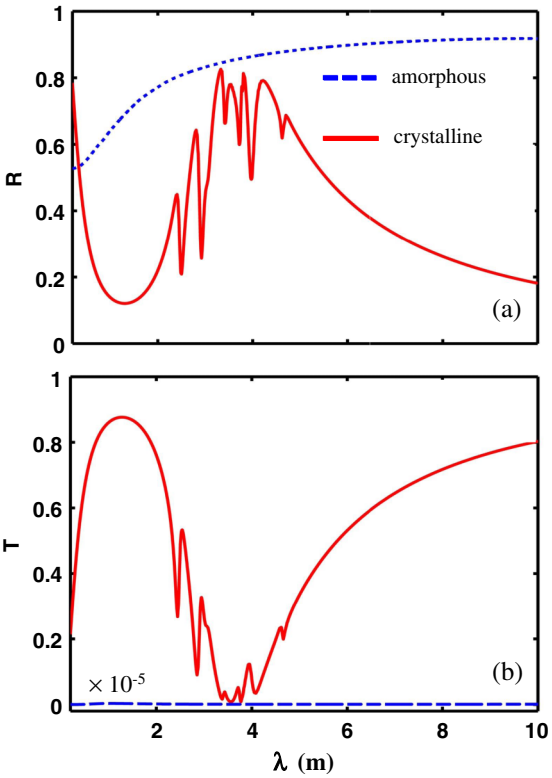

FIG. 2 (color online). (a) Reflectance and (b) transmittance at normal incidence of a 1 μm thick VO_2 membrane in its amorphous (metallic) and crystalline (dielectric) phases. This information is taken from the data of Barker *et al.* [17].

The time evolution of the temperatures T_1 and T_2 of the membranes is a solution of the following nonlinear coupled system of differential equations

$$\partial_t \mathbf{T} = \boldsymbol{\Phi} + \mathbf{Q}, \quad (3)$$

where we have introduced the vectors $\mathbf{T} \equiv (T_1(t), T_2(t))^t$, $\boldsymbol{\Phi} \equiv (\Phi_1(T_1, T_2)/I_1, \Phi_2(T_1, T_2)/I_2)^t$, and $\mathbf{Q} \equiv (Q_1\delta_1/I_1, Q_2\delta_2/I_2)^t$. Here, Q_i $(i = 1, 2)$ is the power per unit volume which can be added to or extracted from both membranes by applying a voltage difference through a couple of electrodes, as illustrated in Fig. 1, or by using Peltier elements. Furthermore, we have introduced the thermal inertia of both membranes as $I_i \equiv C_i \rho_i \delta_i$, where C_i and ρ_i are the heat capacity and the mass density of each material. By writing down this set of equations, we have neglected any temperature variation inside the membranes, which is a very good approximation, given that the conductivity inside the membranes is much larger than between the membranes. When assuming that no energy is directly added to or removed from the membranes, then $\mathbf{Q} = \mathbf{0}$. In this case, the steady-state solution is given by $\boldsymbol{\Phi} = \mathbf{0}$. Hence, Φ_1 and

Φ_2 vanish for the same couple of temperatures $(T_1^{(\text{st-st})}, T_2^{(\text{st-st})})$. Considering for an instant membrane 2 only, then the existence of two equilibrium temperatures where the net flux vanishes ($\Phi_2 = 0$) implies that Φ_2 must have a maximum or a minimum between these two temperatures. Hence, this requires a negative differential resistive behavior for this membrane [8] which was shown for such IMT materials as VO_2 [7]. For the whole system, it is therefore a precondition to have at least one membrane which exhibits negative differential resistive behavior (i.e., VO_2) in order to have two couples $(T_1^{(\text{st-st})}, T_2^{(\text{st-st})})$ of steady-state temperatures.

In Figs. 3(a) and 3(b), we show the time evolutions of two SiO_2/VO_2 systems without external excitation (i.e., $\mathbf{Q} = \mathbf{0}$) when the thermal inertia I_i of both membranes are comparable (i.e., $\delta_1 \approx \delta_2$) and very different (i.e., $\delta_1 \gg \delta_2$). The trajectories (the thick pink and turquoise lines) are obtained by solving Eq. (3) using a Runge-Kutta method with adaptive time steps choosing different initial conditions. In these figures, the dashed blue (solid red) line represents the local equilibrium temperature for the first (second) membrane that is the set of temperature couples (T_1, T_2), which satisfy the condition $\Phi_1(T_1, T_2) = 0$ [$\Phi_2(T_1, T_2) = 0$]. The intersection of these two lines defines the global steady-state temperatures of the system where $\mathbf{\Phi} = \mathbf{0}$. In Fig. 3, we observe three global steady-state temperature couples $(T_1^{(l)}, T_1^{(l)})$ with $l = 1, 2, 3$ for both configurations.

The stability of these steady-state temperatures can be deduced from an analysis of the eigenvalues of the Jacobian of the vector field $\mathbf{\Phi}$. We find [15] that $(T_1^{(1)}, T_2^{(1)})$ and $(T_1^{(3)}, T_2^{(3)})$ are fixed points, whereas $(T_1^{(2)}, T_2^{(2)})$ is a saddle point. It is worth noting that at the fixed points, even in the presence of thermal fluctuations, the system remains in the steady state. Furthermore, it is interesting to see how the system dynamic changes with respect to the thermal inertia I_i of membranes. When $I_1 \sim I_2$, we see in Fig. 3(a) that both membranes simultaneously cool down or heat up toward one of the stable states. On the other hand, if one membrane has a strong inertia with respect to the second one ($I_1 \gg I_2$), we find two time scales for the relaxation toward the steady state, as illustrated in Fig. 3(b). First, the membrane with the smaller inertia reaches its local equilibrium state [defined by $\Phi_2 = 0$ in Fig. 3(b)] by bypassing the unstable state, as shown in Fig. 3(b), and then the whole system relaxes toward a global stable state.

So far, we have identified the stable thermal states $(T_1^{(1)}, T_2^{(1)})$ and $(T_1^{(3)}, T_2^{(3)})$ which can be regarded as the two states 0 and 1 of a bit. Now, we want to examine the transition between these two states. To switch from one thermal state to the other, we need to add or extract power from the system. In the following, we describe this writing-reading procedure. To this end, we consider the SiO_2/VO_2 system made with membranes of equal thicknesses

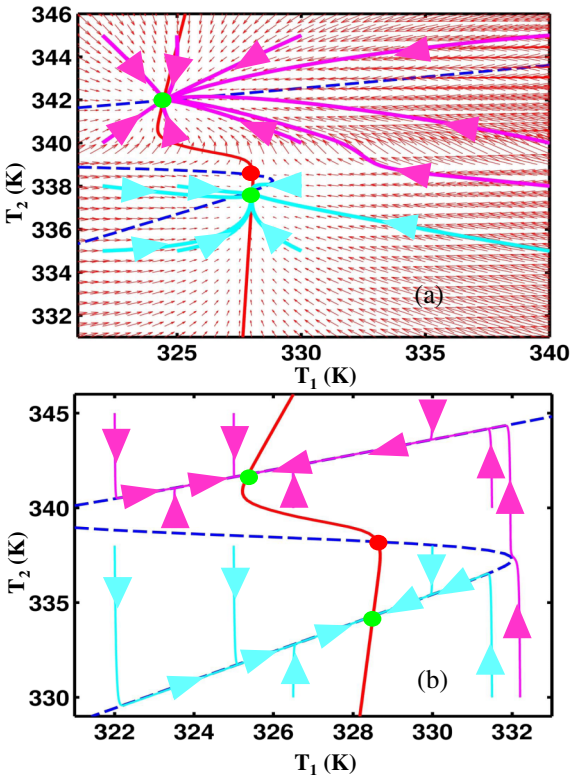

FIG. 3 (color online). (a) Trajectories of temperatures (pink and turquoise lines) for different initial conditions in the plane (T_1, T_2) in a two-membrane SiO_2/VO_2 system with $\delta_1 = \delta_2 = 1$ μm. The dashed blue and solid red lines represent the local equilibrium conditions $\Phi_1 = 0$ and $\Phi_2 = 0$ of each membrane. The green (red) points denote the stable (unstable) global steady-state temperatures $(T_1^{(1)}, T_2^{(1)}) = (328.03\ \text{K}, 337.77\ \text{K})$, $(T_1^{(2)}, T_2^{(2)}) = (328.06\ \text{K}, 338.51\ \text{K})$, and $(T_1^{(3)}, T_2^{(3)}) = (324.45\ \text{K}, 341.97\ \text{K})$. The red arrows in the background represent the vector field $\mathbf{\Phi}$. The temperatures of thermal reservoirs are $T_L = 320$ K and $T_R = 358$ K. (b) Temperature trajectories as in (a) but for a two-membrane SiO_2/VO_2 system with $\delta_1 = 1$ mm and $\delta_2 = 1$ μm, choosing $T_L = 320$ K and $T_R = 355$ K. In both configurations, the separation distance d is much larger than the thermal wavelengths.

$\delta_1 = \delta_2 = 1$ μm, which is coupled to two reservoirs of temperatures $T_L = 320$ K and $T_R = 358$ K. Let us define 0 as the thermal state at the temperature $T_2 = \min(T_2^{(1)}, T_2^{(3)})$. To make the transition toward the thermal state 1, the VO_2 membrane must be heated.

Step 1 (transition from state 0 to state 1): A volumic power $Q_2 = 10^{-2}\ \text{W mm}^{-3}$ is added to this membrane during a time interval $\Delta t_1 \approx 0.4$ s to reach a region in the plane (T_1, T_2) [see Fig. 4(a)] where all trajectories converge naturally (i.e., for $Q_2 = 0$); after some time, toward state 1, the overall transition time is $\Delta t(0 \to 1) = 4$ s [Fig. 4(b)].

Step 2 (maintaining the stored thermal information): Since state 1 is a fixed point, the thermal data can be maintained for an arbitrarily long time, provided that the

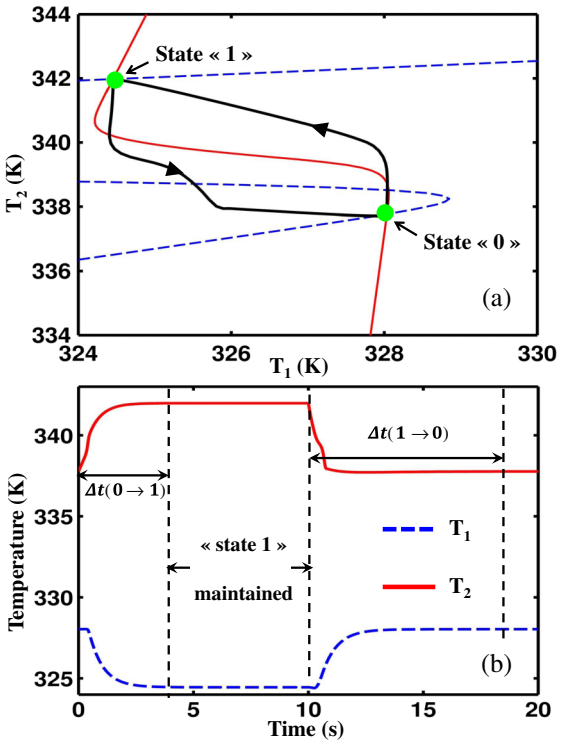

FIG. 4 (color online). (a) Hysteresis of the VO_2 membrane temperature during a transition between the thermal states 0 and 1 inside a two-membrane SiO_2/VO_2 system with $\delta_1 = \delta_2 = 1\ \mu$m. The volumic powers supplied and extracted from the VO_2 layer during time intervals $\Delta t_1 = 0.4$ s and $\Delta t_2 = 1.5$ s are $Q_2 = 10^{-2}\ \mathrm{W\,mm^{-3}}$ and $Q_2 = -2.5 \times 10^{-2}\ \mathrm{W\,mm^{-3}}$, respectively. The writing time of state 1 (0) from state 0 (1) is $\Delta t(0 \to 1) = 4$ s [$\Delta t(1 \to 0) = 8$ s]. (b) Time evolution $T_1(t)$ and $T_2(t)$ of SiO_2 and VO_2 membrane temperatures. The thermal states 0 and 1 can be maintained for an arbitrarily long time, provided that the thermostats ($T_L = 320$ K and $T_R = 358$ K) remain switched on.

thermal reservoirs are switched on. This corresponds basically to the concept of volatile memory in electronics.

Step 3 (transition from state 1 to state 0): Finally, a volumic power $Q_2 = -2.5 \times 10^{-2}\ \mathrm{W\,mm^{-3}}$ is extracted from the VO_2 membrane during a time interval $\Delta t_2 \approx 1.5$ s to reach a region [below $T_2 = 338$ K in Fig. 4(a)] of natural convergence to state 0. In this case, the transition time becomes $\Delta t(1 \to 0) = 8$ s. Compared with its heating, the cooling of VO_2 does not follow the same trajectory [see Fig. 4(a)] outlining the hysteresis of the system which accompanies its bistable behavior. To read out the thermal state of the system, a classical electronic thermometer based on the thermodependence of the electric resistivity of membranes can be used.

In conclusion, we have predicted the existence of bistable thermal behaviors in many-body systems in mutual radiative interaction and we have demonstrated the feasibility for contactless thermal analogs of volatile electronic memories based on this effect which do not require refreshing. In this Letter, our proofs of principle have been established in the far-field regime. Its generalization to the near-field regime is straightforward. Since, at short separation distances, thanks to photon tunneling, the heat flux exchanged between both membranes is not limited by the Stefan-Boltzmann law anymore but can be increased by orders of magnitude, the speed of natural cooling or heating could also be drastically increased. We think that the radiative thermal memories pave the way for a contactless treatment of heat flows. They could find broad applications in the domains of thermal management, information processing, and energy storage.

The authors acknowledge financial support by the DAAD and Partenariat Hubert Curien Procope Program (Project No. 55923991). P. B.-A. acknowledges financial support by the Agence Nationale de la Recherche through the Source-TPV Project ANR 2010 BLANC 0928 01 and thanks Professor H. Benisty for fruitful discussions.

*pba@institutoptique.fr

[1] B. Li, L. Wang, and G. Casati, Appl. Phys. Lett. **88**, 143501 (2006).
[2] L. Wang and B. Li, Phys. Rev. Lett. **99**, 177208 (2007).
[3] L. Wang and B. Li, Phys. Rev. Lett. **101**, 267203 (2008).
[4] N. Li, J. Ren, L. Wang, G. Zhang, P. Hänggi, and B. Li, Rev. Mod. Phys. **84**, 1045 (2012).
[5] C. R. Otey, W. T. Lau, and S. Fan, Phys. Rev. Lett. **104**, 154301 (2010).
[6] P. Ben-Abdallah and S.-A. Biehs, Appl. Phys. Lett. **103**, 191907 (2013).
[7] P. Ben-Abdallah and S.-A. Biehs, Phys. Rev. Lett. **112**, 044301 (2014).
[8] L. Zhu, C. R. Otey, and S. Fan, Appl. Phys. Lett. **100**, 044104 (2012).
[9] P. Ben-Abdallah, S.-A. Biehs, and K. Joulain, Phys. Rev. Lett. **107**, 114301 (2011).
[10] R. Messina, M. Antezza, and P. Ben-Abdallah, Phys. Rev. Lett. **109**, 244302 (2012).
[11] R. Messina and M. Antezza, Phys. Rev. A **89**, 052104 (2014).
[12] S. M. Rytov, Y. A. Kravtsov, and V. I. Tatarskii, *Principles of Statistical Radiophysics* (Academy of Sciences of USSR, Moscow, 1953), Vol. 3.
[13] D. Polder and M. Van Hove, Phys. Rev. B **4**, 3303 (1971).
[14] R. Messina and M. Antezza, Phys. Rev. A **84**, 042102 (2011).
[15] See Supplemental Material at http://link.aps.org/supplemental/10.1103/PhysRevLett.113.074301 for a detailed calculation of heat flux exchanges in a two-membrane system.
[16] M. M. Qazilbash, M. Brehm, B. G. Chae, P.-C. Ho, G. O. Andreev, B. J. Kim, S. J. Yun, A. V. Balatsky, M. B. Maple, F. Keilmann, H. T. Kim, and D. N. Basov, Science **318**, 1750 (2007).
[17] A. S. Barker, H. W. Verleur, and H. J. Guggenheim, Phys. Rev. Lett. **17**, 1286 (1966).
[18] P. J. van Zwol, K. Joulain, P. Ben-Abdallah, and J. Chevrier, Phys. Rev. B **84**, 161413(R) (2011).
[19] *Handbook of Optical Constants of Solids*, edited by E. Palik (Academic, New York, 1998).